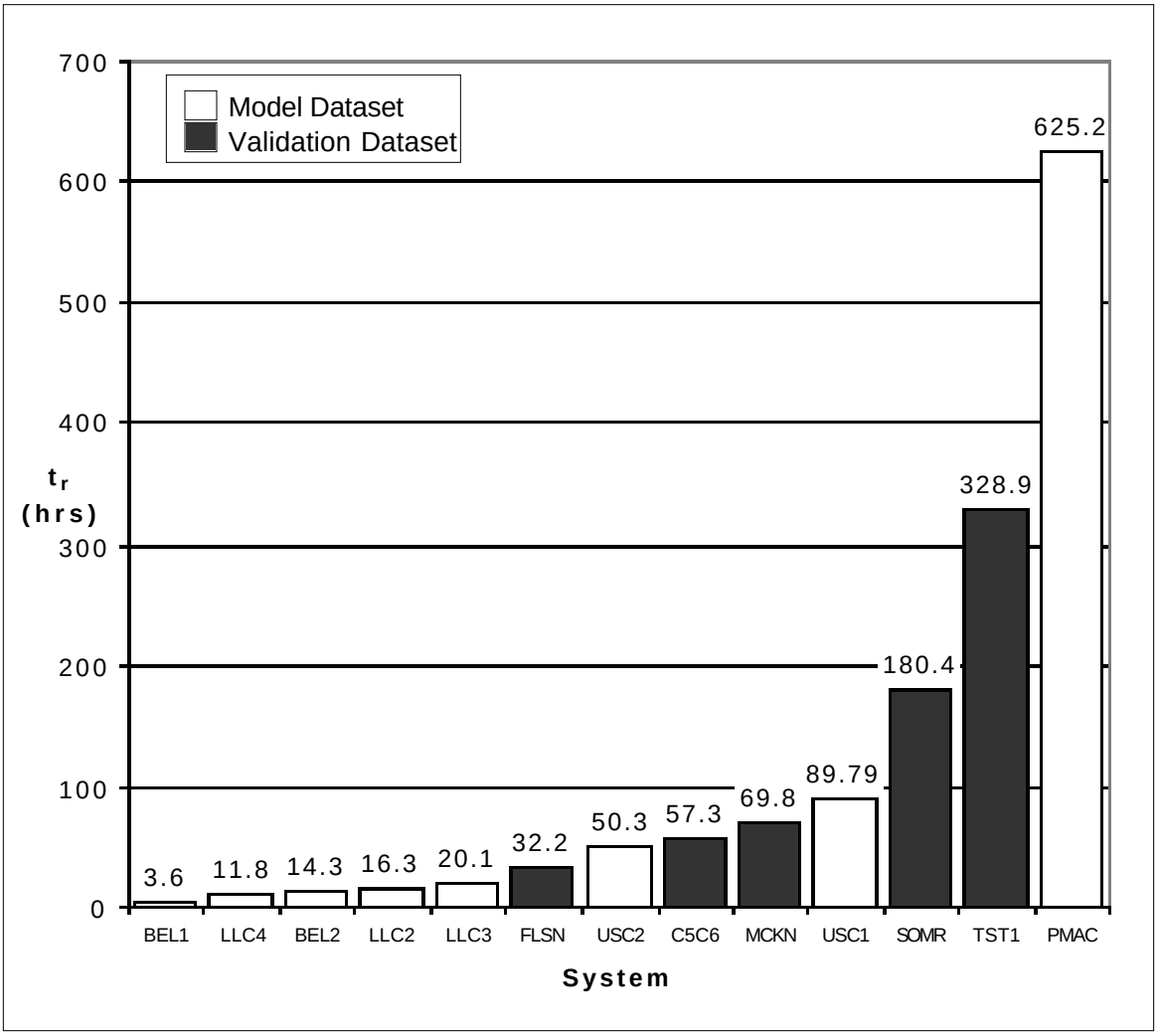

Figure 3.11 Histogram of the mean residence times for the SAPS systems in the model and calibration data sets.

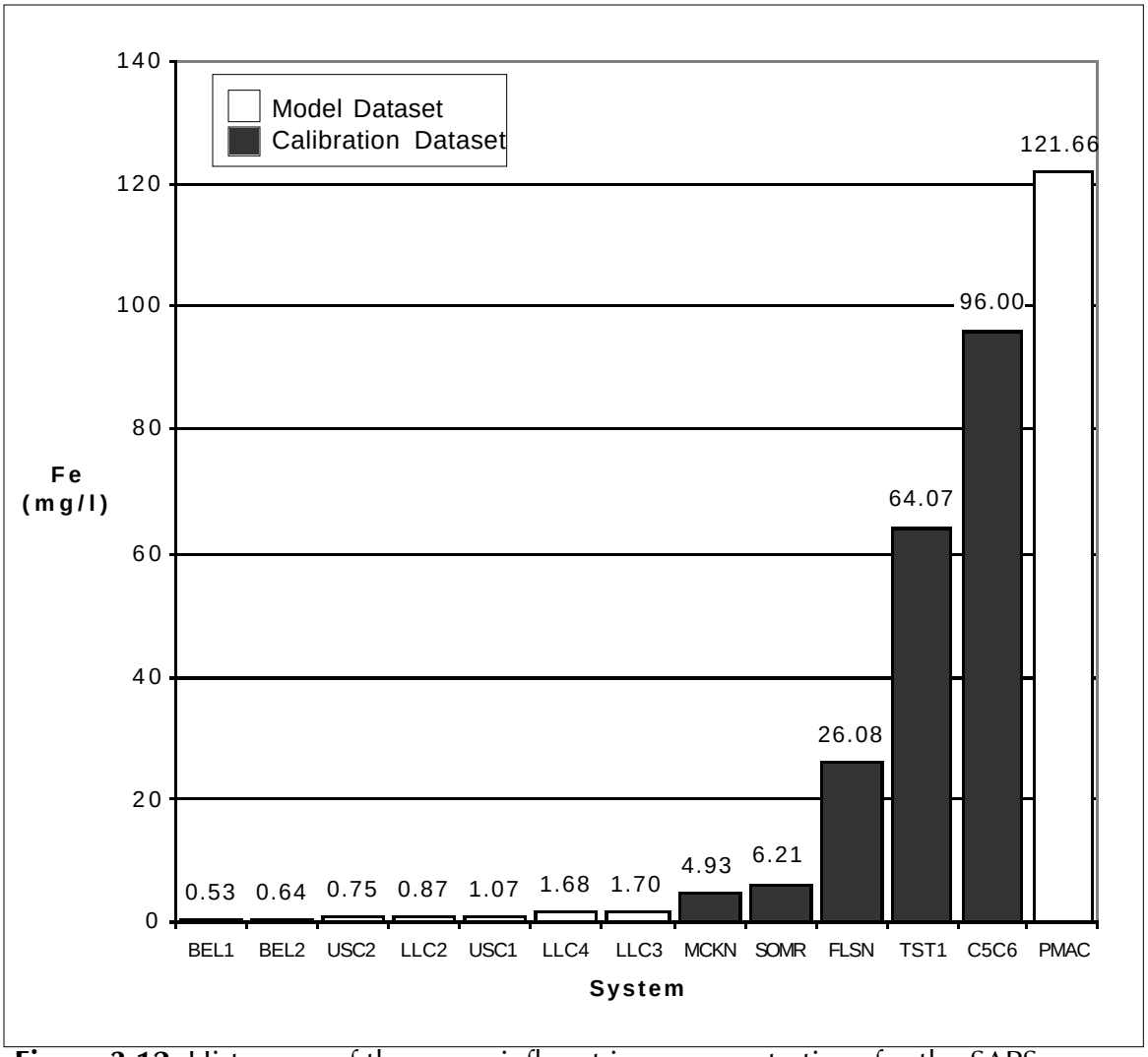

Figure 3.12 Histogram of the mean influent iron concentrations for the SAPS systems in the model and calibration data sets.

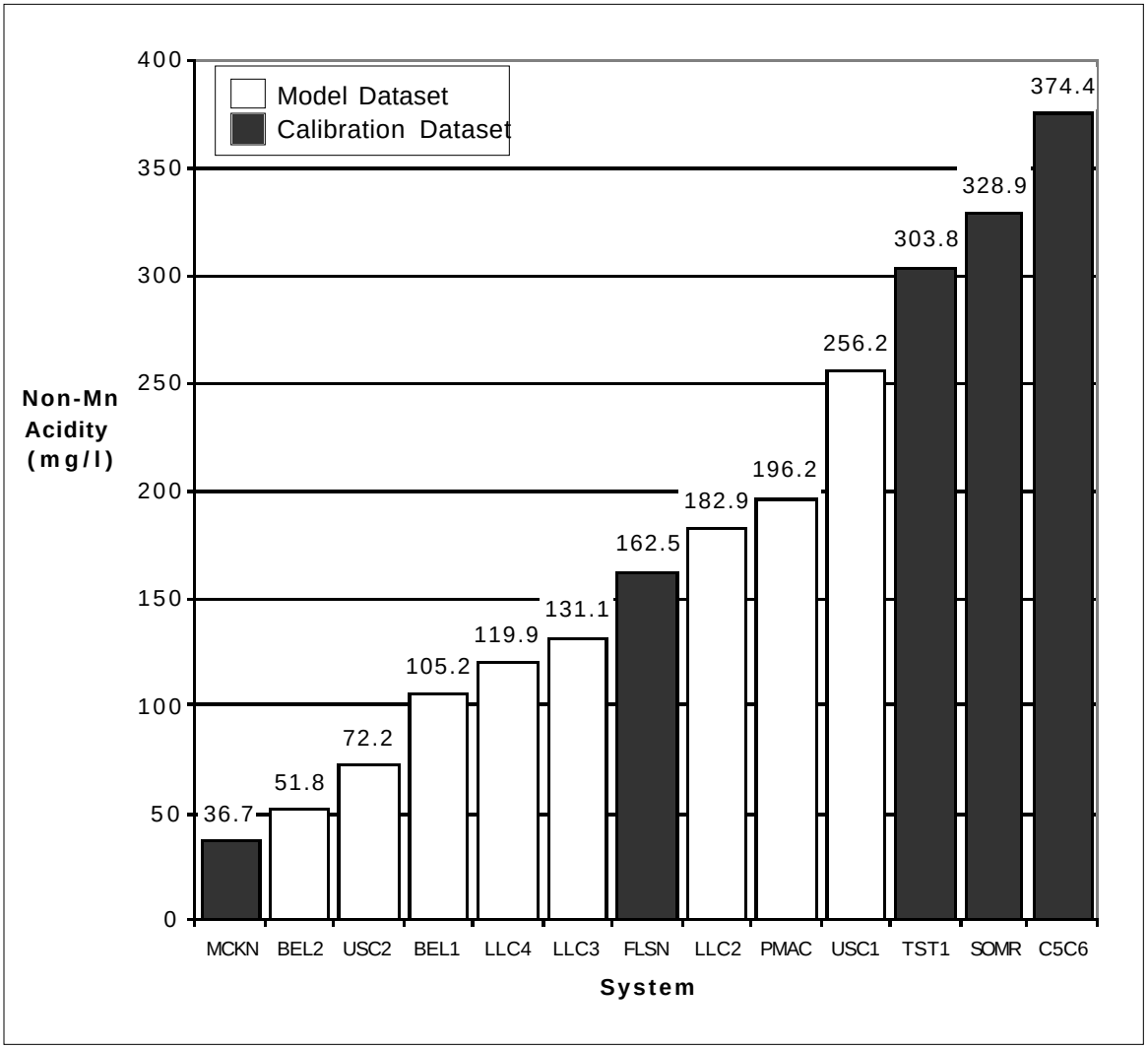

Figure 3.13 Histogram of the influent non-Mn Acidity for the SAPS systems in the model and calibration data sets. Values represent $CaCO_3$ equivalent.

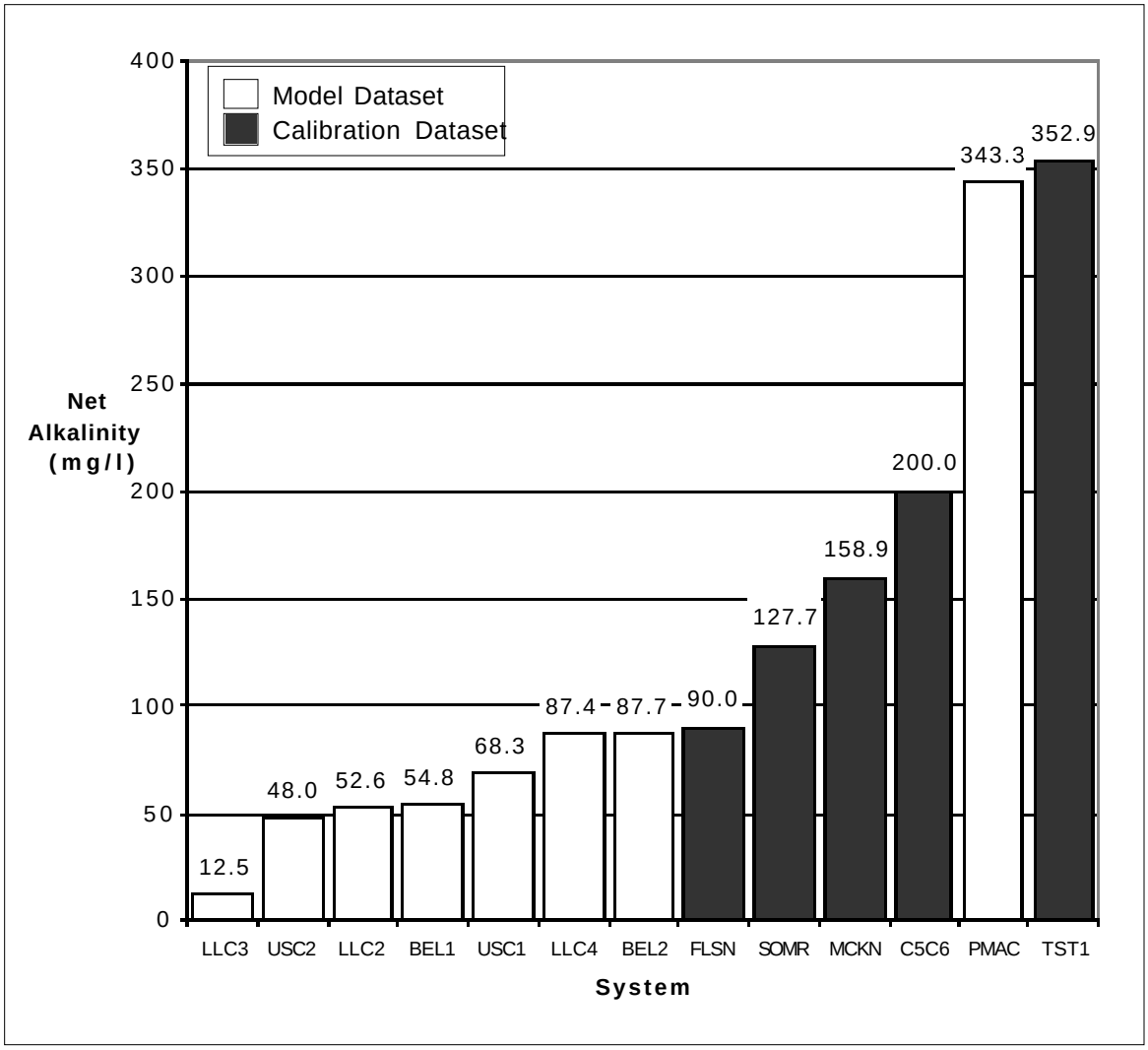

Figure 3.14 Histogram of the net alkalinity generation for the SAPS systems in the model and calibration data sets. Values represent $CaCO_3$ equivalent.

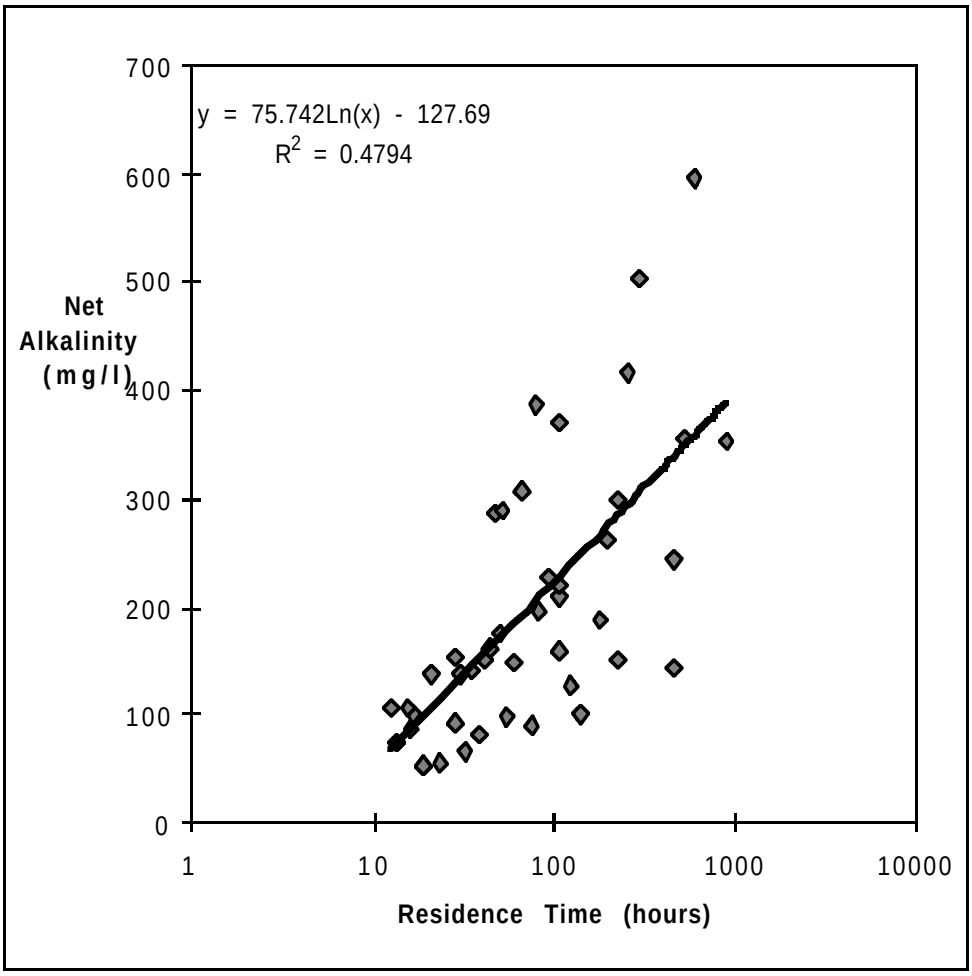

Figure 3.15 Relationship between AMD residence time in the limestone layer and net alkalinity generation for the calibration data set. Net alkalinity values reflect $CaCO_3$ equivalent. n=45

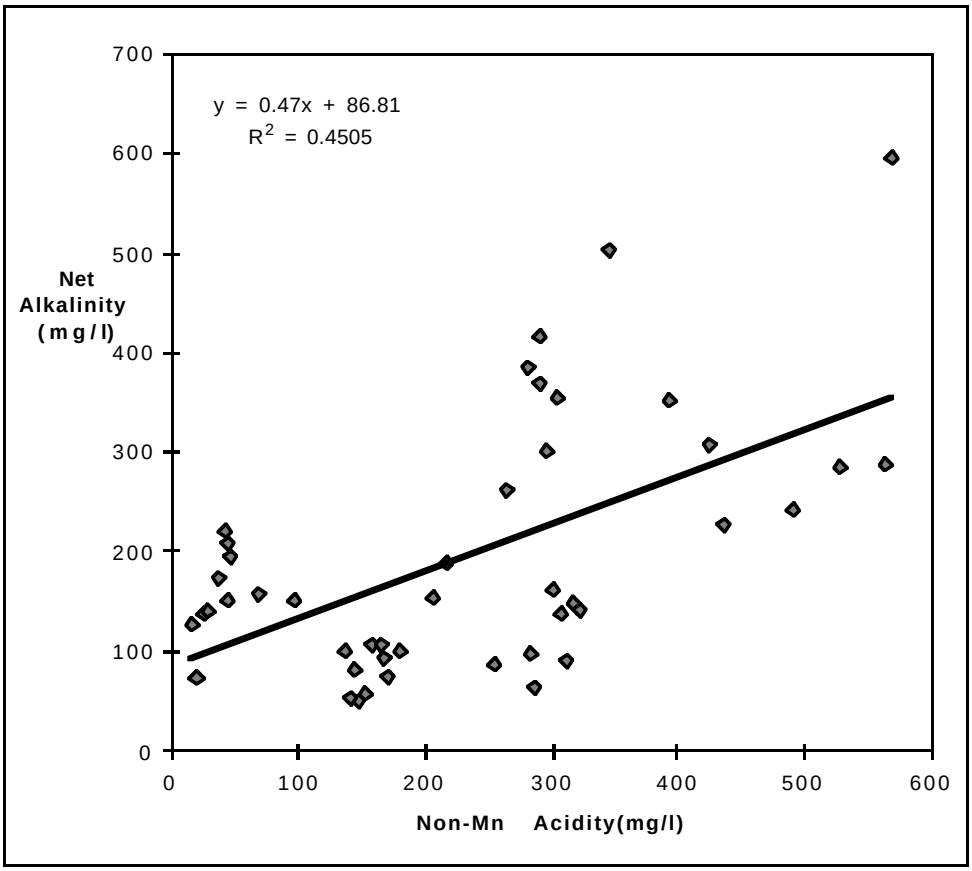

Figure 3.16 Relationship between influent non-Mn acidity and net alkalinity generation for the calibration data set. Values reflect $CaCO_3$ equivalent. n=45

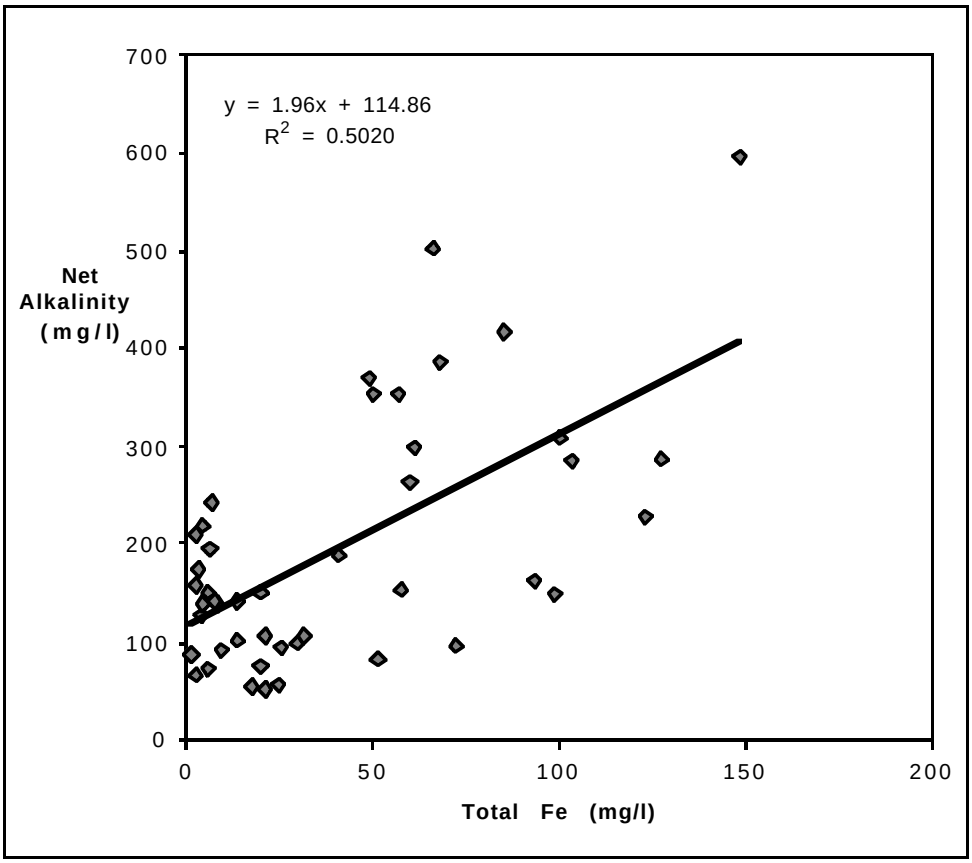

Figure 3.17 Relationship between total influent iron and net alkalinity generation for the calibration data set. Net alkalinity values reflect $CaCO_3$ equivalent. n=45

combined both of the sets of the data. This data set was manipulated to change the weighted proportion of each of the data sets that was to be regressed.

Nine regressions were performed using the calibration-data/model-data weighted proportions of 10/90, 20/80, 30/70, 40/60, 50/50, 60/40, 70/30, 80/20, and 90/10. The parameter estimates of each iteration of the regression were then used to model both sets of data independently. The final parameter estimates selected at the 50/50 proportion for several reasons. First, they reflected an equal compromise of the two data sets. Secondly, they were in a stable region of proportions that resulted in little parameter change. And finally, they maintained high R-squared values (Table 3.7) (Birch, 1999). The SAS code used in calculating these relationships is presented in Appendix A. This resulted in the following model for net alkalinity generation for a SAPS cell. As with the original, this model was

Net Alkalinity (mg/l as $CaCO_3$) =

$$43.12\ln(t_r) + 0.75Fe + 0.23\text{Non-Mn Acidity} - 58.45 \qquad (3.5)$$

to produce a slope of 1 by multiplying the equation by 1.376 resulting in the final model:

Net Alkalinity (mg/l as $CaCO_3$) =

$$59.33\ln(t_r) + 1.03Fe + 0.32\text{Non-Mn Acidity} - 80.43 \qquad (3.6)$$

To examine the accuracy of the model, predicted net alkalinities were generated for each set of influent sampling events, and plotted versus the actual net alkalinity recorded in the field. When using the original data set, the observed versus predicted results were highly correlated (R^2=0.7491), as would be expected (Figure 3.18). When using the independent data set, the model's prediction accuracy still

proved to be significant (R^2=0.6279) (Figure 3.19). The combined data sets are illustrated in figure 3.20, yielding an over all R-squared value of 0.7217.

The 95% confidence limits were calculated for the data set to determine prediction accuracy. These values are point specific but range from ±79.44 to ±87.06 mg/l as $CaCO_3$ of net alkalinity. Since this model was derived empirically, it is not intended to be extrapolated beyond the original range of data and such predictions could be subject to error.

Model Assessment

The final model is able to predict the ability of SAPS to generate net alkalinity with a high degree of statistical significance (R^2 =0.7217). Model terms conform to current understanding of carbonate equilibria. The positive logarithmic relationship exhibited by residence time and net alkalinity is logical in that the rate of limestone dissolution will slow with time as the water reaches saturation with respect to calcite (Rose, 1999). The relationship between influent iron and net alkalinity generation is seen in part as a function of the acidity derived from iron oxidation and hydrolysis. For systems receiving large amounts of ferric iron or that have long residence times, iron is able to hydrolyze and precipitate in the open water of the SAPS, forming proton acidity (Hedin et al., 1994b). When this acidity is drawn into the limestone, it increases the rate of limestone dissolution (Rose, 1999).

The non-Mn acidity is related to net alkalinity in a similar fashion as iron but for a different reason. This parameter takes into account the fraction of total acidity that is able to be neutralized in systems that are only capable of raising the pH to circumneutral levels. For this reason, it demonstrates the same positive relationship as iron. This parameter, however, is viewed as a proxy for the lack of aluminum,

Table 3.7 Parameter estimates and R-squared values from each of the weighted proportion runs used to calibrate the SAPS alkalinity generation model.

Proportion Calibration/ Model	$\ln(t_r)$	Fe	Acidity	Intercept	Combined R-squared	Model R-squared	Calibration R-squared
10/90	54.16	1.04	0.10	-99.18	0.6571	0.7103	0.6598
20/80	50.25	0.89	0.14	-84.12	0.6613	0.7238	0.6523
30/70	47.40	0.82	0.17	-73.25	0.6697	0.7333	0.6449
40/60	45.10	0.78	0.20	-64.93	0.6801	0.7413	0.6368
50/50	43.12	0.75	0.23	-58.40	0.6918	0.7490	0.6273
60/40	41.36	0.73	0.26	-53.31	0.7047	0.7566	0.6156
70/30	39.73	0.71	0.30	-49.52	0.7191	0.7646	0.6010
80/20	38.16	0.68	0.36	-47.11	0.7358	0.7732	0.5822
90/10	36.62	0.65	0.43	-46.43	0.7565	0.7802	0.5575

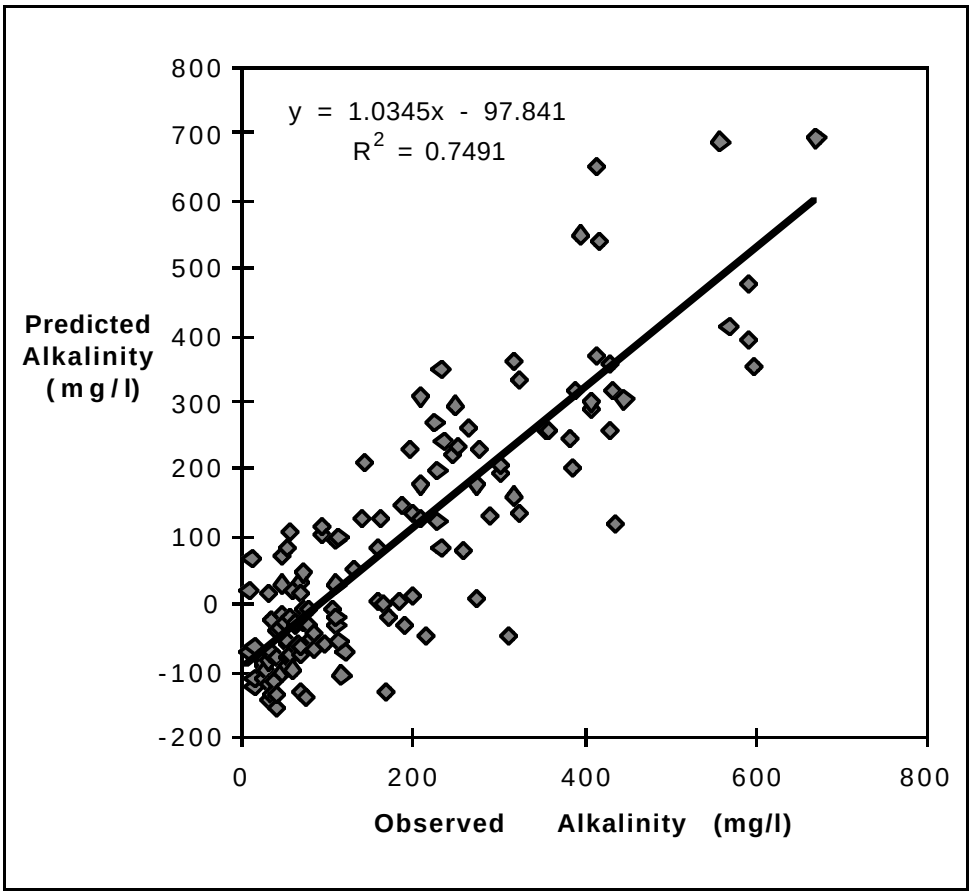

Figure 3.18 Relationship between observed and predicted values for the SAPS net alkalinity generation model using the model data set. Values reflect $CaCO_3$ equivalent. n=135

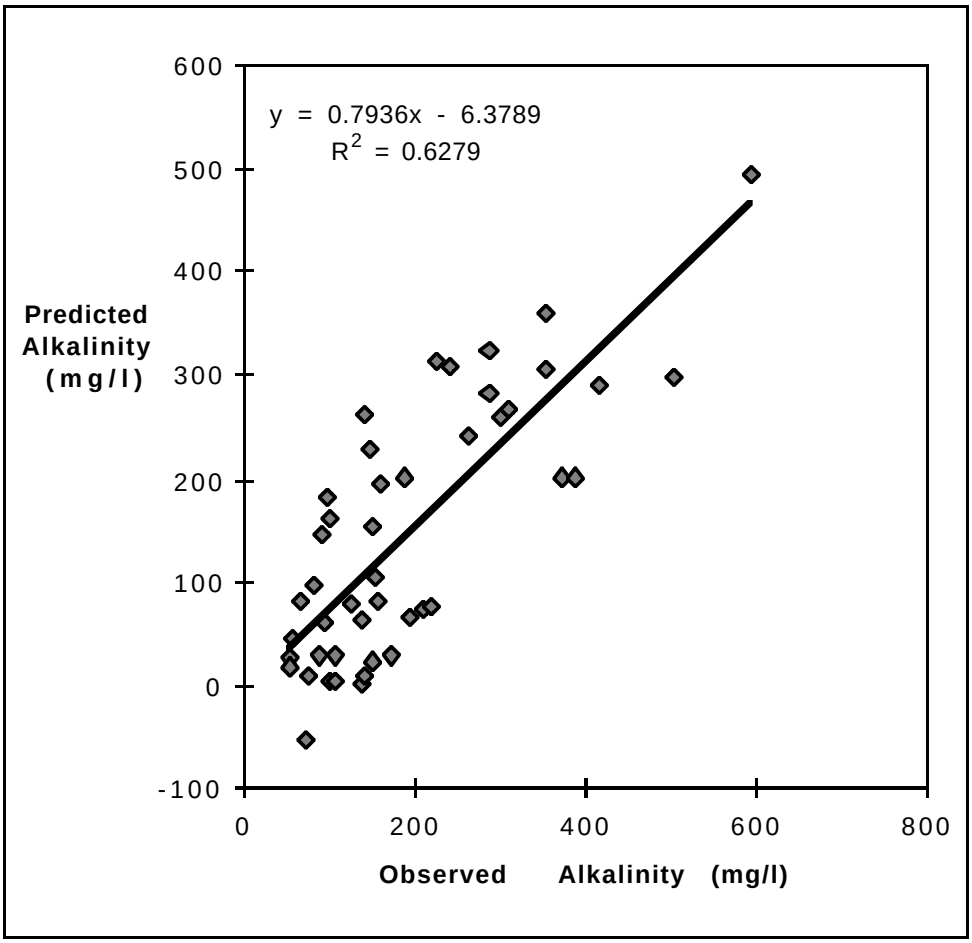

Figure 3.19 Relationship between observed and predicted values for the SAPS net alkalinity generation model using the calibration data set. Values reflect $CaCO_3$ equivalent. n=45

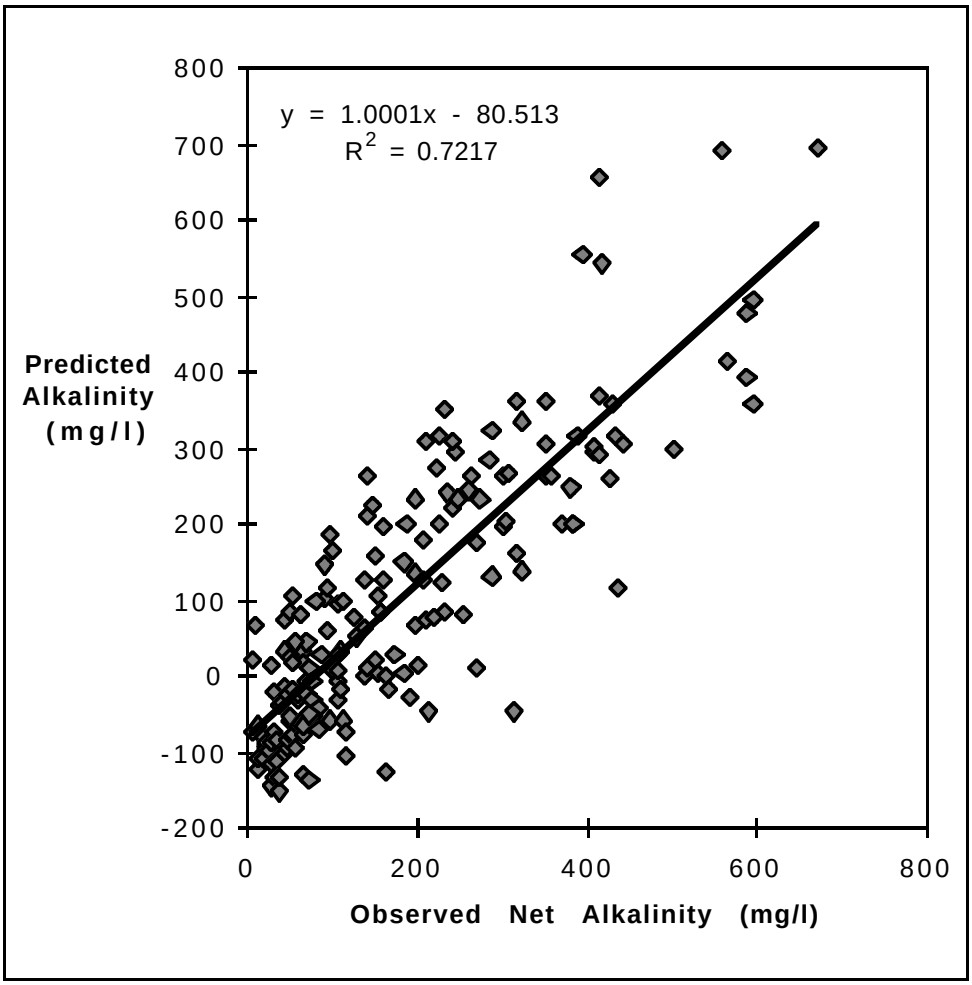

Figure 3.20 Relationship between observed and predicted values for the SAPS net alkalinity generation model using the combined data sets. Values reflect $CaCO_3$ equivalent. n=180

ferrous iron, and ferric iron data. If such data were available, it is believed that a better accounting of the effect that the individual metal species on system performance would be possible and a term such as non-Mn acidity would be necessary. The fact that this parameter includes the acidity that results from iron hydrolysis called for caution to be used in its selection in order to avoid multicollinearity with the iron term in the model.

The correlation between total iron and non-Mn acidity for the entire data set was r=0.4598. This degree of correlation did not meet our criterion for exclusion based on multicollinearity (r>0.9). One explanation for the lack of correlation between iron and non-Mn acidity is the influence of aluminum on system performance. The influence of non-Mn acidity can be viewed as the variation in aluminum-derived acidity over and above the iron acidity. This is because aluminum is the most prevalent source of mineral acidity in coal mine drainage that was not directly accounted for in this study. Therefore, this variation is viewed as the contribution of this term to overall model which is evidenced by its improvement of the model R-squared value by 0.0577.

A second source of variation between iron and non-Mn acidity could be a result of the ferrous / ferric iron ratio in the AMD. Since the two species can generate different amounts of acidity, the ratio of the two would dictate the net acidity derived from the total iron concentration. There is the assumption, however, that 100% of the iron's mineral acidity will be expressed as proton acidity. The procedure for measuring total acidity quantifies the acidity that is generated from the complete oxidation of all metal species in solution. In the field, there are other mechanisms which can remove iron from solution with out expressing its mineral acidity. One such example is with formation of siderite which is common when ferrous iron comes in to contact with limestone (Eq. 3.7).

$$Fe^{2+} + CaCO_3 \rightarrow Ca^{2+} + FeCO_3 \quad (3.7)$$

To improve the accuracy of this model and account for the role of mineral acidity in SAPS, a more complete metals analysis which includes aluminum, ferric iron, and ferrous iron concentrations should be performed and modeled to determine the influence of each parameter on system performance.

Conclusions

• The generation of net alkalinity by SAPS is controlled by both residence time and influent water chemistry.

• The response of alkalinity generation to residence time is logarithmic, as the rate of alkalinity generation is at first rapid, but decreases over time. This is due to the decreasing dissolution rate of limestone as the water approaches saturation with respect to calcite.

• Non-manganese acidity is a more accurate predictor of net alkalinity generation than total acidity.

• Net alkalinity generation by SAPS increases in response to increasing levels of iron and non-manganese acidity.

• The net alkalinity generation for a SAPS system can be adequately predicted by:

Net Alkalinity (mg/l as $CaCO_3$) =

$$59.33\ln(t_r) + 1.03Fe + 0.32\text{Non-Mn Acidity} - 80.43$$

where t_r is the theoretical retention time in hours, Fe is the concentration of total influent iron in mg/l, and Non-Mn Acidity is the non-manganese acidity in mg/l as $CaCO_3$.

• Future research in modeling the performance of SAPS should include the effect of influent aluminum and the ferrous/ ferric iron ratio on net alkalinity generation.